Light scattering in fractals with scalar and bond-bending models

1997 J. Phys.: Condens. Matter 9 2149

(http://iopscience.iop.org/0953-8984/9/10/005)

J. Phys.: Condens. Matter **9** (1997) 2149–2164. Printed in the UK PII: S0953-8984(97)77529-5

Light scattering in fractals with scalar and bond-bending models

Abdelali Rahmani†‖, Claude Benoit‡, Rémi Jullien§, Gérard Poussigue‡ and Abdellah Sakout†

† Laboratoire d'Optique et de Spectroscopie, Faculté des Sciences, Dhar Mehraz, BP 1796, Atlas-Fès, Morocco

‡ Groupe de Dynamique des Phases Condensées, Unité Mixte de Recherches CNRS 5581, Université Montpellier II, place Eugène Bataillon, 34095 Montpellier Cédex 5, France

§ Laboratoire des Verres, UMR 5587 CNRS, Université Montpellier II, place Eugène Bataillon, 34095 Montpellier Cédex 5, France

Received 4 September 1996

Abstract. We have computed the Raman scattering intensity for very large bond-percolating clusters and diffusion-limited cluster–cluster aggregates in three dimensions. Using the spectral moments method, we considered both scalar and bond-bending potentials to model interactions between atoms of our fractal systems. We assumed that scattering was produced either by the dipole-induced dipole (DID) or by the bond-polarizability mechanisms. The results have been analysed in terms of the light scattering scaling theory and compared with the experimental Raman scattering data obtained for silica aerogels. We found that the DID mechanism applied to the diffusion-limited cluster–cluster aggregation model gives a good description of the Raman scattering in base-catalysed silica aerogels.

1. Introduction

In recent years, there had been growing interest in the dynamic properties of porous media. This was stimulated by theoretical work on vibrational excitations in fractal structures (Alexander and Orbach 1982). These investigations revealed that vibrational excitations of weakly connected fractal systems consist of localized low-energy modes, called fractons. Their density of states (DOS) $g(\omega)$ was assumed to scale with the frequency ω as

$$g(\omega) \sim \omega^{\tilde{d}-1} \tag{1}$$

where the spectral dimension $\tilde{d}$ differs from the Euclidean dimension d. The fractons are characterized by a length scale λ related to ω, D and $\tilde{d}$ by

$$\lambda(\omega) \sim \omega^{-\tilde{d}/D}. \tag{2}$$

The first measurements of the low-frequency Raman scattering intensity for silica aerogels were obtained by Boukenter *et al* (1986, 1987). Interaction of fractons with light gives rise to a Raman scattering intensity, assumed to be written as

$$\frac{I(\omega)}{n(\omega)+1} = \frac{C(\omega)g(\omega)}{\omega} \sim \omega^{\nu} \tag{3}$$

‖ Permanent address: Département de Physique, Université Kaddi Ayad, Faculté des Sciences et Techniques, BP 618, Gheliz-Marrakech, Morocco.

0953-8984/97/102149+16$19.50

where $C(\omega)$ describes the coupling between vibrational modes and photons, $n(\omega)$ is the Bose factor and ν is a scaling index. They analysed their results, assuming the ensemble-averaged form for the fracton wavefunctions introduced by Alexander *et al* (1985), which is generally incorrect (Keys and Ohtsuki 1987).

To detect fractons, several experiments have been carried out on silica aerogels (Courtens *et al* 1987, 1988, Tsujimi *et al* 1988, Vacher *et al* 1988, 1990, Pelous *et al* 1992). The very-low frequency inelastic polarized and depolarized scattering of light from vibrations of these systems was studied and the results analysed on the basis of scaling considerations based on the fracton model. Pelous *et al* (1992) observed that two domains can be distinguished in a broad frequency domain around the lowest-frequency Raman-active modes (about 10 cm^{-1}) of the silica aerogel particles. At very low frequencies (much less than 10 cm^{-1}), they observed a regime with ν-values varying between -0.4 and -0.8, depending on the catalysis conditions of the aerogel preparation. On the other hand, in the 100–150 cm^{-1} range, a coefficient $\nu > +0.3$ has been obtained. The physical origin of these modes is still a matter of discussion.

These experiments have stimulated further theoretical developments. In particular, a general analysis of light scattering from fractals has been developed on the basis of scaling assumptions (Alexander 1989, Alexander, Courtens and Vacher (ACV) 1993). In these studies, it is postulated that all average lengths that can be defined on fractons, either wavelength, scattering length or localization length, scale with the fracton frequency as in equation (2). In other words all these lengths are the same apart from numerical constants. This statement is called the single-length-scale postulate (SLSP). To interpret the experimental results obtained for silica aerogels, several mechanisms which can lead to light scattering have been proposed: the direct mechanism which is related to the change in mass distribution in the fracton regime, the dipole-induced dipole (DID) mechanism which takes care of dipolar radiation, and the Pockel effect which expresses the fluctuations in the particle polarizabilities due to strains in these particles.

To check the scaling indices entering this light theory, many computed experiments have been carried out. Montagna *et al* (1990), Pilla *et al* (1992) and Mazzacurati *et al* (1992) have numerically calculated polarized Raman scattering for the DID effective polarizability model of the site-percolating (SP) cluster built on 65×65 lattices for $d = 2$, and on $29 \times 29 \times 29$ lattices for $d = 3$. Their results suggest that the theoretical predictions of ACV are not valid. Stoll *et al* (1992) have computed the Raman coupling coefficient $C(\omega)$ for the DID scattering process for SP and bond-percolating (BP) clusters in two and three dimensions. Their results concerning BP clusters revealed that the scattering is extremely sensitive to granularity and their computed scaling exponents support the theoretical predictions. A very different scaling was observed in the case of SP clusters (Montagna *et al* 1990, Stoll *et al* 1992). In order to clarify these discrepancies, Viliani *et al* (1995) have calculated the Raman scattering coupling coefficient $C(\omega)$ for both SP and BP systems in two and three dimensions. Their results disagree with the scaling theory. In agreement with equation (7), Terao and Nakayama (1996) found that, for BP networks in three dimensions, the Raman scattering intensity follows a power law with the exponent σ close to unity. Benoit *et al* (1992b) have calculated the Raman intensity of a disordered Sierpinski gasket. The results confirm that, in the fracton regime, the Raman intensity behaves according to a power law, and the value of the exponent ν depends on the susceptibility derivatives.

The aim of this paper is twofold: first, we study, for several structures and force field models, the scaling behaviour of light scattering for the DID and bond-polarizability (BPOL) mechanisms; second, we try to interpret the experimental results concerning Raman scattering from silica aerogels at the light of the vectorial elasticity model. We have studied

polarized and depolarized light scattering from percolating clusters and diffusion-limited cluster–cluster aggregates (DLCAs) built in $d = 3$ (Hasmy *et al* 1994). Both scalar and three-body forces are considered. In the following, we first review the scaling arguments and different processes of light scattering. We then present the dynamic models that we used, and finally we discuss the results obtained.

2. Scaling arguments

The first analysis of the experimental Raman scattering results obtained for silica aerogels were based on an ensemble-averaged form for the fracton wavefunctions. Indeed, Alexander *et al* (1985, 1986) assume that the amplitude of the normalized wavefunction associated with a fracton of frequency ω and located at a distance r has the following form:

$$\Phi(\omega, r) \sim \lambda^{-D/2} \exp[-\tfrac{1}{2}(r/\lambda)^{d_\phi}] \tag{4}$$

where λ is the localization length, which obeys equation (2), and d_ϕ is a geometrical exponent describing the localization in real space.

Considering that the local strain induced by the fracton ω is proportional to the gradient of the wavefunction Φ, the reduced intensity of light scattered at a point by a fracton localized at a distance r obeys equation (3), with

$$\nu = \frac{\tilde{d}}{D}(2d_\phi + D) - 2. \tag{5}$$

The validity of this analysis was criticized by Keys and Ohtsuki (1987). To avoid errors induced by the ensemble-averaged form of the wavefunction idea, Alexander *et al* (1993) have developed a general formalism for light scattering from fractals. Based on the SLSP, they found that the intensity scales with ω, with indices that depend on the assumed scattering mechanism.

In the light scattering experiment, the incident electric field $\boldsymbol{E}_i$ creates a polarization $\boldsymbol{P}(\boldsymbol{r}, t)$, given by

$$\boldsymbol{P}(\boldsymbol{r}, t) \sim \tilde{\chi}\boldsymbol{E}_i(\boldsymbol{r}, t) \tag{6}$$

where $\tilde{\chi}$ is the dielectric susceptibility tensor. The scattering intensity depends on the fluctuations $\delta\boldsymbol{P}$ of the polarization.

2.1. Direct mechanism

The particles are rigid. Polarization fluctuations are due to density fluctuations. The scattering intensity is thus directly proportional to the correlation function or the dynamic structure factor which was considered in previous studies (Rahmani *et al* 1995, 1996). The intensity defined in equation (3) must follow, in the $q\lambda \ll 1$ limit, the following scaling relation:

$$\frac{I_{dir}(\omega)}{n(\omega) + 1} \sim \omega^{-2\tilde{d}(2-\sigma)/D-2} \tag{7}$$

where σ is a scaling index describing the modulation of the mass distribution by the vibration.

2.2. Dipole-induced dipole mechanism

The polarization of neighbouring particles gives rise to an internal field $\boldsymbol{E}_{ind}$ at a given particle in addition to the average macroscopic field $\boldsymbol{E}_i$.

In this approach, the local field in each particle forming the material is then given by

$$\boldsymbol{E}_{loc} = \boldsymbol{E}_i + \boldsymbol{E}_{ind} \tag{8}$$

where $\boldsymbol{E}_{ind}$ is the field due to all the mean dipole moments $\boldsymbol{P}_n$ induced directly by the field $\boldsymbol{E}_i$ in each particle n. Particle displacements involve the polarization fluctuations $\delta\boldsymbol{P}_{ind}$, which is taken to be proportional to the induced field (Montagna *et al* 1990):

$$\delta\boldsymbol{P}_{ind}(\boldsymbol{r}_n, t) \sim \chi_n\, \delta\boldsymbol{E}_{ind}(\boldsymbol{r}_n, t) \tag{9}$$

with

$$\delta\boldsymbol{E}_{ind}(r_n, t) = \delta\left(\sum_{n'} \tilde{\mathbf{T}}(\boldsymbol{r}(t)_{nn'})\boldsymbol{P}_n(\boldsymbol{r}'_n, t) \right) \tag{10}$$

with the dipolar interaction tensor given by

$$\tilde{\mathbf{T}}(\boldsymbol{r}) = [\boldsymbol{r} \otimes \boldsymbol{r} - \tfrac{1}{3}\mathbf{1}r^2]/r^5. \tag{11}$$

$\delta\boldsymbol{E}_{ind}(\boldsymbol{r}_n, t)$ represents fluctuations of the created field at a point $\boldsymbol{r}_n$ by the average dipole moment $\boldsymbol{P}_{n'}$ located at a point $\boldsymbol{r}_{n'}$. Hence, if we assume that the polarizability of particles is constant, the polarization fluctuations can be written as

$$\delta\boldsymbol{P}_{ind}(r_n, t) = \delta\tilde{\pi}^n \cdot \boldsymbol{E}_i(\boldsymbol{r}_{n'}, t) \tag{12}$$

where the components of the tensor polarizability $\tilde{\pi}^n$ are defined by

$$\pi^n_{\alpha\gamma}(t) = \sum_{n'} \chi_n \chi_{n'} T_{\alpha\gamma}(\boldsymbol{r}_{nn'}(t)). \tag{13}$$

As shown by Alexander *et al* (1993), one can distinguish the high-frequency limit ($q\lambda \ll 1$), where the long-range coherence of the strains is important, and the low-frequency limit ($q\lambda \gg 1$), which is dominated by short-range dipolar coupling and by the fluctuating local strains.

In the $q\lambda \ll 1$, one can show that the long-range contribution of the DID (LRDID) mechanism to intensity would follow the power law (equation (3))

$$\frac{I_{LRDID}(\omega)}{n(\omega)+1} \sim \omega^{-2\tilde{d}(D-d-\sigma)/D-2}. \tag{14}$$

The DID mechanism, truncated to nearest neighbours (NNDID), gives rise to an incoherent contribution which complies with the scaling

$$\frac{I_{NNDID}(\omega)}{n(\omega)+1} \sim \omega^{2\tilde{d}\sigma/D+\tilde{d}-2}. \tag{15}$$

The exponent σ in this latter equation can differ from the σ in equation (14) and can take a value smaller than one. The polarizability tensor is given by

$$\pi^n_{\alpha\gamma}(t) = \sum_{\substack{n' \\ \langle nn \rangle}} \boldsymbol{\chi}_n \boldsymbol{\chi}_{n'} T_{\alpha\gamma}(\boldsymbol{r}_{nn'}(t)) \tag{16}$$

where $\langle nn \rangle$ indicates that n and n' are nearest neighbours.

If we consider that this polarization is only modulated if the nearest neighbours are connected by a bond, one obtains the BPOL contribution. The tensor polarizability is then given by

$$\pi^n_{\alpha\gamma}(t) = \sum_{\substack{n' \\ \langle nn \rangle}} K_{nn'} T_{\alpha\gamma}(\boldsymbol{r}_{nn'}(t)) \tag{17}$$

where $K_{nn'} = 1$, if n and n' are connected, and $K_{nn'} = 0$ otherwise. The BPOL contribution is identical with the NNDID contribution for SP and DLCA models.

3. Models

3.1. Light scattering

The scattered light in a given direction, with a frequency between ω_f and $\omega_f + \mathrm{d}\omega_f$ and a solid angle $\mathrm{d}\Omega$, is related to the differential scattering cross section, which is given by Poussigue *et al* (1991), with $q \approx 0$:

$$\frac{\mathrm{d}^2\sigma}{\mathrm{d}\Omega\,\mathrm{d}\omega_f} = \frac{1}{8\pi^2 c^2}\omega_f^3 \omega_i (n(\omega)+1)\hbar \sum_i \sum_{\alpha\gamma\beta\lambda} n^i_\alpha n^i_\beta H_{\alpha\gamma\beta\lambda}(\omega) l_\gamma l_\lambda \tag{18}$$

where

$$H_{\alpha\gamma\beta\lambda}(\omega) = \sum_j a^*_{\alpha\gamma}(j) a_{\beta\lambda}(j) \frac{1}{2\omega_j}[\delta(\omega-\omega_j) - \delta(\omega+\omega_j)] \tag{19}$$

with

$$a_{\alpha\gamma}(j) = \sum_{m\delta} \frac{\pi^m_{\alpha\gamma,\delta}}{\sqrt{m_m}} e_j(m\delta). \tag{20}$$

ω_i is the frequency of the incident light, $\boldsymbol{n}^i$ $(i = 1, 2)$ and $\boldsymbol{l}$ are the polarization unit vectors for scattered and incident light, respectively; $\boldsymbol{n}^1$ and $\boldsymbol{n}^2$ are two mutually perpendicular unit vectors that are both perpendicular to the direction of propagation of the light, m_n is the mass of the nth atom and $e_j(n\delta)$ is the $(n\delta)$ component of the jth mode. Coefficients $\pi^m_{\alpha\gamma,\delta}$ connect the polarization fluctuations to particle motions. They are obtained by expanding the polarizability tensor $\tilde{\pi}^n$ in terms of particle displacements u^δ_m, with

$$\pi^m_{\alpha\gamma,\beta} = \sum_n \left(\frac{\partial \pi^n_{\alpha\gamma}}{\partial u^\delta_m}\right)_0 \tag{21}$$

where $\pi^n_{\alpha\gamma}$ are given by equations (13), (16) and (17) for DID, NNDID and BPOL mechanisms, respectively. The polarized Raman scattering corresponds, for example, to $\boldsymbol{E}_i = |\boldsymbol{E}_i|\boldsymbol{x}$ and $\boldsymbol{n}^1 // \boldsymbol{x}$ ($\alpha = \beta = \gamma = \lambda = 1$ in equation (18)). Depolarized Raman scattering is obtained with $\boldsymbol{n}^2 // \boldsymbol{y} \perp \boldsymbol{x}$ ($\alpha = \beta = 2$; $\gamma = \lambda = 1$).

Using the spectral moments method (Benoit *et al* 1992a), we calculate a symmetrical function $I_{\alpha\gamma}(\omega)/(n(\omega)+1)$, which is equal, apart from a constant factor, to the differential scattering cross section (18), for $\omega > 0$:

$$\begin{aligned} \frac{I_{\alpha\gamma}(\omega)}{n(\omega)+1} &= \sum_j \frac{|a_{\alpha\gamma}(j)|^2}{2\omega_j}(\delta(\omega-\omega_j) + \delta(\omega+\omega_j)) \\ &= \sum_j |a_{\alpha\gamma}(j)|^2 \delta(\omega^2 - \omega_j^2). \end{aligned} \tag{22}$$

3.2. Dynamic models

In this paper, we consider two models: scalar and vectorial models. In the vectorial model, the potential takes into account vector displacements, and is given by (Feng, 1985a, b)

$$V = \tfrac{1}{2}\alpha \sum_{\langle nm \rangle} [(\boldsymbol{u}_n - \boldsymbol{u}_m) \cdot \boldsymbol{r}_{nm}]^2 K_{nm} + \tfrac{1}{2}\beta \sum_{\langle mnl \rangle} (\delta\theta_{mnl})^2 K_{nm} K_{nl} \tag{23}$$

where α and β are the central and the bond-bending force constants, respectively, $\boldsymbol{u}_n$ is the (infinitesimal) displacement of site n and $\boldsymbol{r}_{nm}$ is a unit vector from site n to site m. K_{nm} is a bond parameter between n and m, where $K_{nm} = 1$ if both sides n and m are occupied by atoms and otherwise $K_{nm} = 0$. $\langle mnl \rangle$ indicates that the sum is over all triplets in which the bonds $\langle mn \rangle$ and $\langle nl \rangle$ form an angle whose vertex is at n, and $\delta\theta_{mnl}$ is the small change in angle between bonds $\langle nm \rangle$ and $\langle nl \rangle$ due to the atom displacements. If the bending of collinear bonds, i.e. bonds that are 180° to one another, is also allowed, then (Sahimi and Arbabi 1993)

$$\delta\theta_{mnl} = \begin{cases} (\boldsymbol{u}_{nm} \times \boldsymbol{r}_{nm} - \boldsymbol{u}_{nl} \times \boldsymbol{r}_{nl}) \cdot (\boldsymbol{r}_{nm} \times \boldsymbol{r}_{nl}) / |\boldsymbol{r}_{nm} \times \boldsymbol{r}_{nl}| & \boldsymbol{r}_{nm} \text{ not parallel to } \boldsymbol{r}_{nl} \\ |(\boldsymbol{u}_{nm} + \boldsymbol{u}_{ne}) \times \boldsymbol{r}_{nm}| & \boldsymbol{r}_{nm} \text{ parallel to } \boldsymbol{r}_{nl} \end{cases} \tag{24}$$

where $\boldsymbol{u}_{nm} = \boldsymbol{u}_n - \boldsymbol{u}_m$. We now report the results obtained for light scattering with these models.

4. Numerical results

As mentioned above, several studies have been carried out to find a scaling law for Raman scattering in fractals. We propose a very large simulation of the Raman scattering for three-dimensional (3D) BP networks and 3D DLCAs. Assuming that the scattering DID and BPOL mechanisms are involved, we consider that atoms first interact via the scalar model and secondly via the bond-bending interacting model. We note that all figures below are plotted on the decimal log–log scale.

4.1. Scalar model

In figure 1, we report, polarized DID (xx-DID), depolarized DID (xy-DID) and BPOL spectra for a 3D BP system at $p_c = 0.248$. The linear size of the system is $L = 85$ and the number of sites is 226 940. We observe a power-law dependence with exponents $\nu = -0.41 \pm 0.02$, $\nu = -0.45 \pm 0.02$ and $\nu = 0.95 \pm 0.02$ for xx-DID, xy-DID and BPOL, respectively (table 1)

In figures 2(a), 2(b) and 2(c), we present xx-DID, xy-DID and BPOL spectra respectively, for three 3D DLCA samples; these three samples, denoted samples A-DLCA, B-DLCA and C-DLCA have concentrations $c = 0.050$, $c = 0.075$ and $c = 0.150$, respectively. The linear size of the clusters is $L = 100$. We see that, for the three cases, the low-frequency Raman intensity follows a nice power law with an exponent depending on the concentrations for the DID mechanism (table 1). The exponent ν varies from 0.45 (0.26) to 0.52 (0.37) when the concentration increases from 0.05 to 0.15 for xx-DID (xy-DID). In the case of the BPOL mechanism, the exponent ν is equal to 0.77 for samples A-DLCA, B-DLCA and C-DLCA samples.

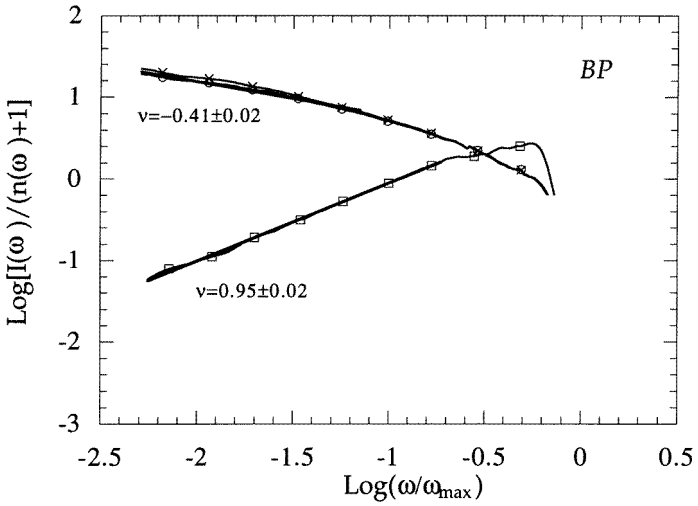

Figure 1. Log–log plot of Raman scattering intensity $I(\omega)/[n(\omega)+1]$ versus ω for the 3D BP system with scalar elasticity for the DID and BPOL mechanisms: —○—, xx-DID; —×—, xy-DID; —□—, BPOL. The straight lines are fits with the indicated slopes.

Table 1. The exponent ν, deduced from the spectrum, in the case of the scalar model for BP and DLCA models using DID and BPOL mechanisms.

	ν		
Model	xx-DID	xy-DID	BPOL
BP	-0.41 ± 0.02	-0.45 ± 0.02	0.95 ± 0.02
A-DLCA	0.52 ± 0.02	0.37 ± 0.02	0.77 ± 0.02
B-DLCA	0.47 ± 0.02	0.33 ± 0.02	0.77 ± 0.02
C-DLCA	0.45 ± 0.02	0.26 ± 0.02	0.77 ± 0.02

4.2. Tensorial model

In earlier studies (Feng 1985a, b, Yakubo and Nakayama 1990), it was found that for the percolating networks model, with rotationally invariant elastic forces, there was a crossover length scale l_c, which depended on the relative strength of the microscopic bond-stretching and bond-bending elastic force constants. For length $l > l_c$, the vibrational DOS of fractons is governed by a spectral dimension $\tilde{D} \approx 0.8$–0.9 (equation (1)). For length $l < l_c$, the bond-stretching motion would be dominant and the DOS fractons are characterized by the conjectured value $\tilde{d} = 4/3$.

To take into account the vector nature of the realistic systems, we consider the potential defined in equation (23). Before presenting the Raman scattering results obtained for 3D BP and 3D DLCA systems, we report the DOSs obtained for these systems. In figures 3(a) and 3(b) we show the results for the DOS spectra for the BP system at $p = p_c$ and for the DLCA at $c = 0.075$ (sample B-DLCA), respectively. The ratio β/α takes the values 0.01 (open circles), 0.10 (open squares) and 1.00 (open triangles). The straight lines, for $\beta/\alpha = 0.01$, in the low-frequency region of the spectra, indicate the slopes 0.00 and -0.10 for the BP and DLCA systems, respectively.

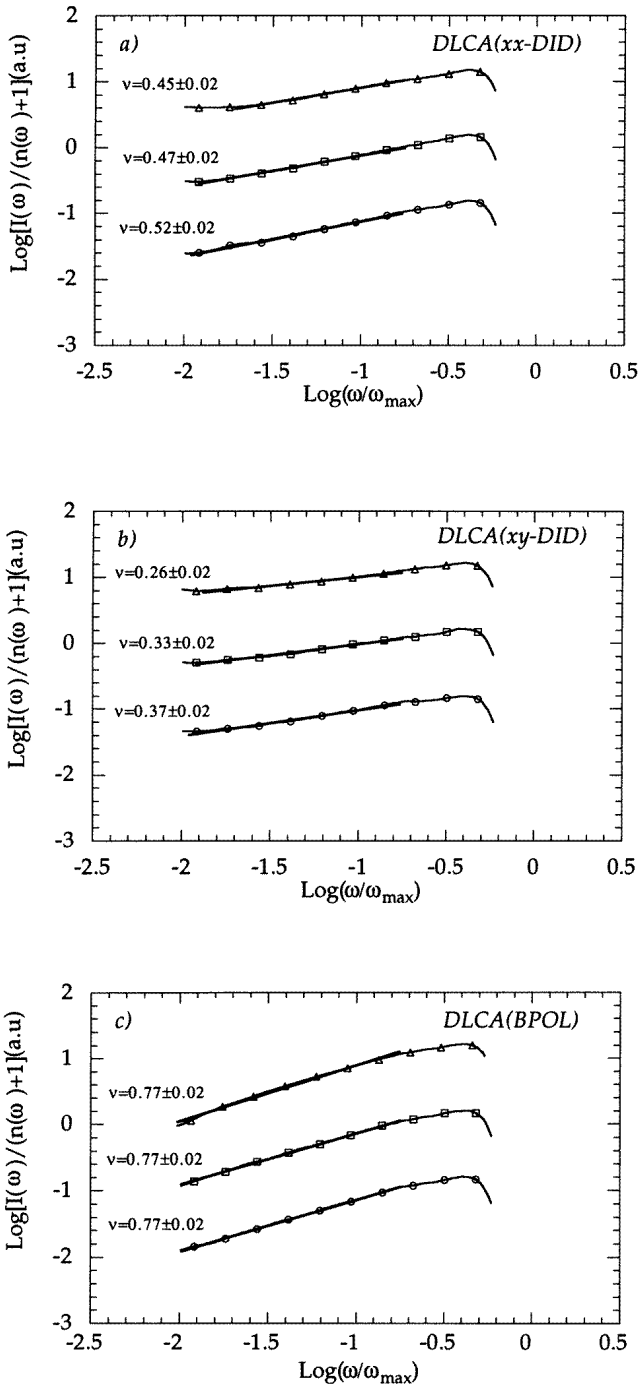

Figure 2. Log–log plot of Raman scattering intensity $I(\omega)/[n(\omega)+1]$ versus ω for the three aggregates A-DLCA ($c = 0.05$) (○), B-DLCA ($c = 0.075$) (□) and C-DLCA ($c = 0.15$) (△) for scalar elasticity: (*a*) xx-DID; (*b*) xy-DID; (*c*) BPOL. The straight lines are fits with indicated slopes.

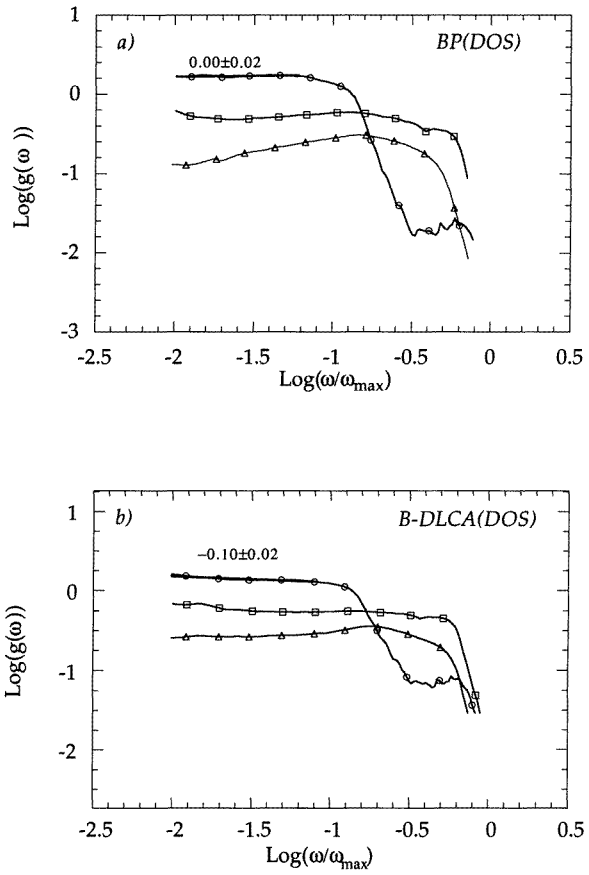

Figure 3. Log–log plot of DOS $g(\omega)$ versus ω/ω_{max} for the (a) BP and (b) the B-DLCA systems for tensorial elasticity for the ratio $\beta/\alpha = 0.01$ (○), 0.10 (□) and 1.00 (△). ω_{max} is the maximal frequency of the spectra. The straight lines are fits with the indicated slopes.

The corresponding values of the bond-bending fracton dimension are $\tilde{D} \approx 1.0$ for percolating systems and $\tilde{D} \approx 0.9$ for the DLCA. These values agree with the predicted value $\tilde{D} \approx 0.8$–0.9.

In figure 4, we report the Raman scattering intensity spectra obtained for BP systems for different values of the ratio β/α : 0.01 (○), 0.10 (□) and 1.00 (△). Figures 4(a) and 4(b) show the results for the xx-DID and xy-DID mechanisms, respectively. We observe that for $\beta/\alpha = 0.01$, for which the bond-bending forces are dominant, Raman scattering follows a power law with exponents $\nu = -1.03 \pm 0.02$ (xx-DID) and $\nu = -0.93 \pm 0.02$ (xy-DID). Figure 4(c) shows the results obtained with the BPOL mechanism, for the two values $\beta/\alpha = 0.01$ and 0.10, open symbols for xx-BPOL and full symbols for xy-BPOL. The scaling behaviour appears only in the case of xx-BPOL with a scaling exponent $\nu = -1.35 \pm 0.02$.

In figures 5–7, we have plotted the spectra of the Raman scattering intensity for samples A-DLCA, B-DLCA and C-DLCA, respectively. In the case of DID, for each sample, the results for polarized and depolarized spectra are given for three values of the ratio

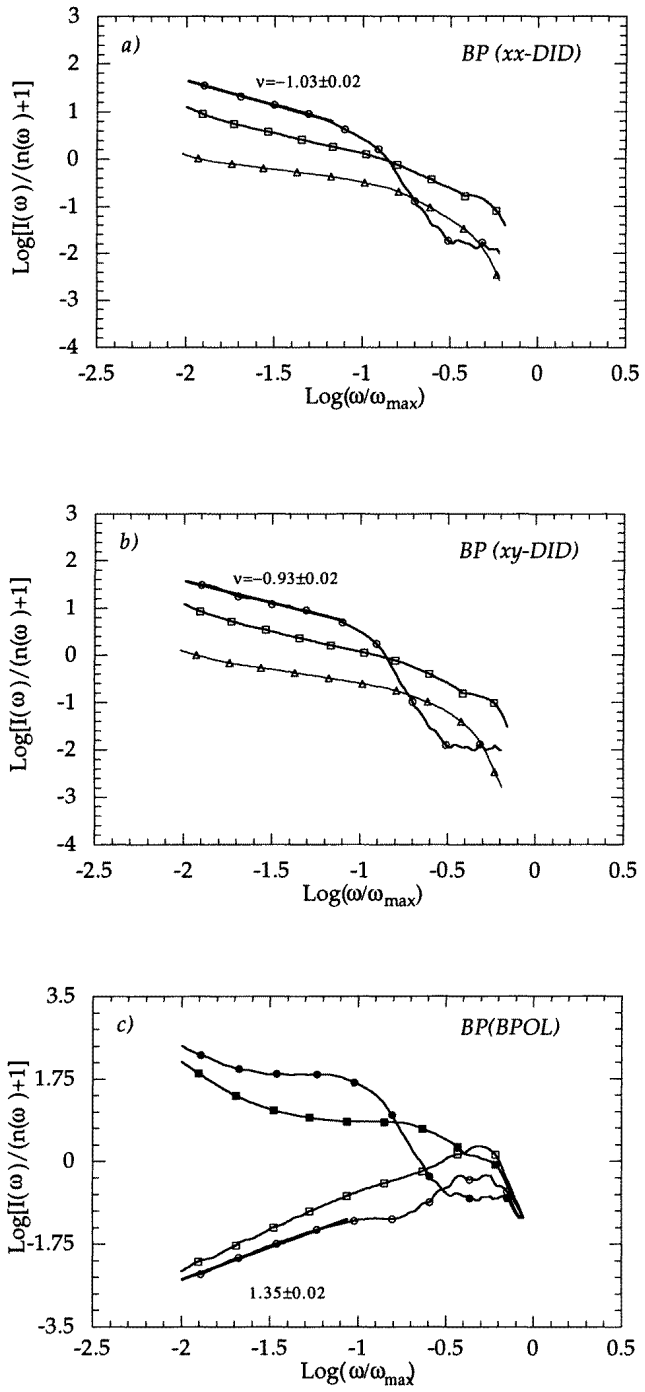

Figure 4. Log–log plot of Raman scattering intensity $I(\omega)/[n(\omega)+1]$ versus ω/ω_{max} for the 3D BP system for tensorial elasticity for $\beta/\alpha = 0.01$ (○, ●), 0.10 (□, ■) and 1.00 (△): (*a*) *xx*-DID; (*b*) *xy*-DID; (*c*) *xx*-BPOL (○, □) and *xy*-BPOL (●, ■). ω_{max} is the maximal frequency of the spectra. The straight lines are fits with the indicated slopes.

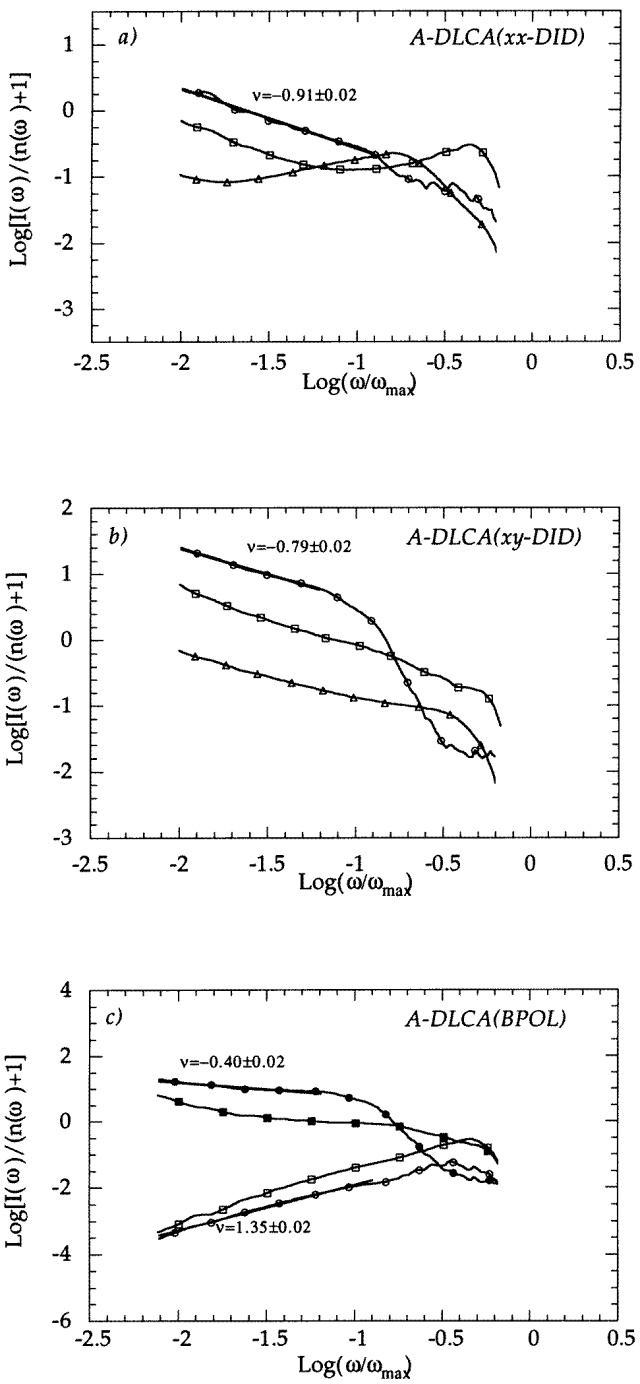

Figure 5. Log–log plot of Raman scattering intensity $I(\omega)/[n(\omega)+1]$ versus ω/ω_{max} for the A-DLCA system for tensorial elasticity for $\beta/\alpha = 0.01$ (○, ●), 0.10 (□, ■) and 1.00 (△): (*a*) *xx*-DID; (*b*) *xy*-DID; (*c*) *xx*-BPOL (○, □) and *xy*-BPOL (●, ■). ω_{max} is the maximal frequency of the spectra. The straight lines are fits with the indicated slopes.

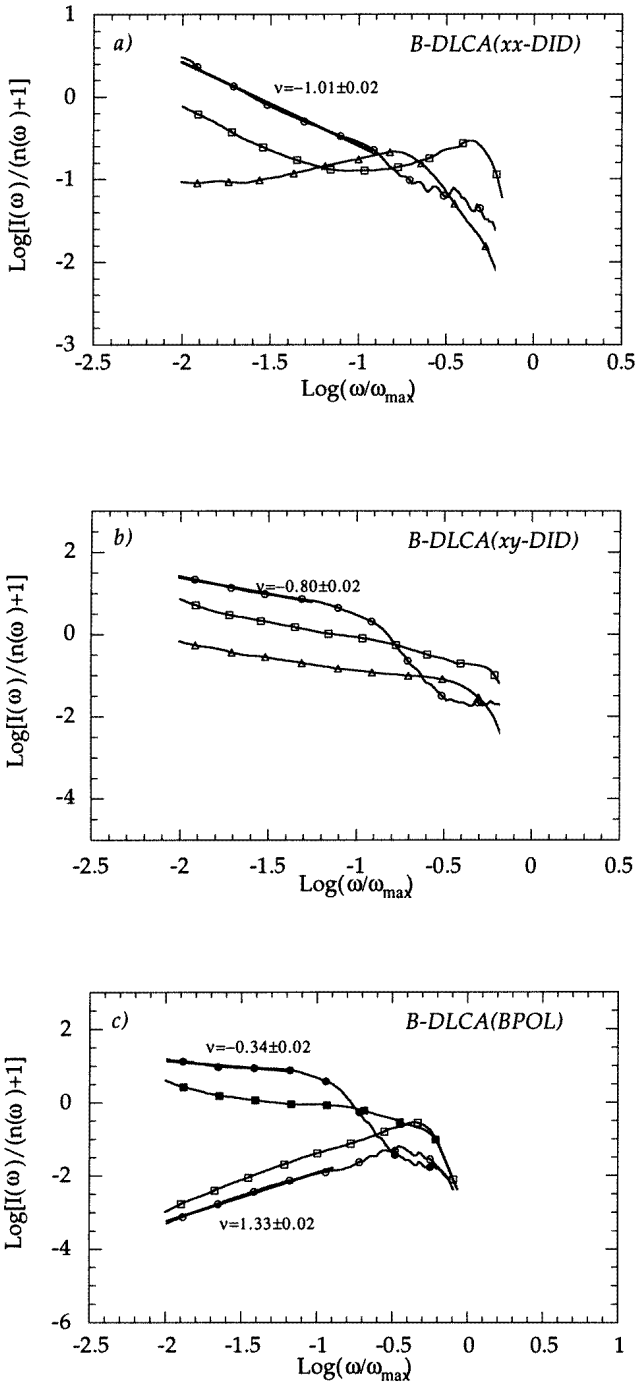

Figure 6. Log–log plot of Raman scattering intensity $I(\omega)/[n(\omega)+1]$ versus ω/ω_{max} for the B-DLCA system for tensorial elasticity for $\beta/\alpha = 0.01$ (○, ●), 0.10 (□, ■) and 1.00 (△): (*a*) *xx*-DID; (*b*) *xy*-DID; (*c*) *xx*-BPOL (○, □) and *xy*-BPOL (●, ■). ω_{max} is the maximal frequency of the spectra. The straight lines are fits with the indicated slopes.

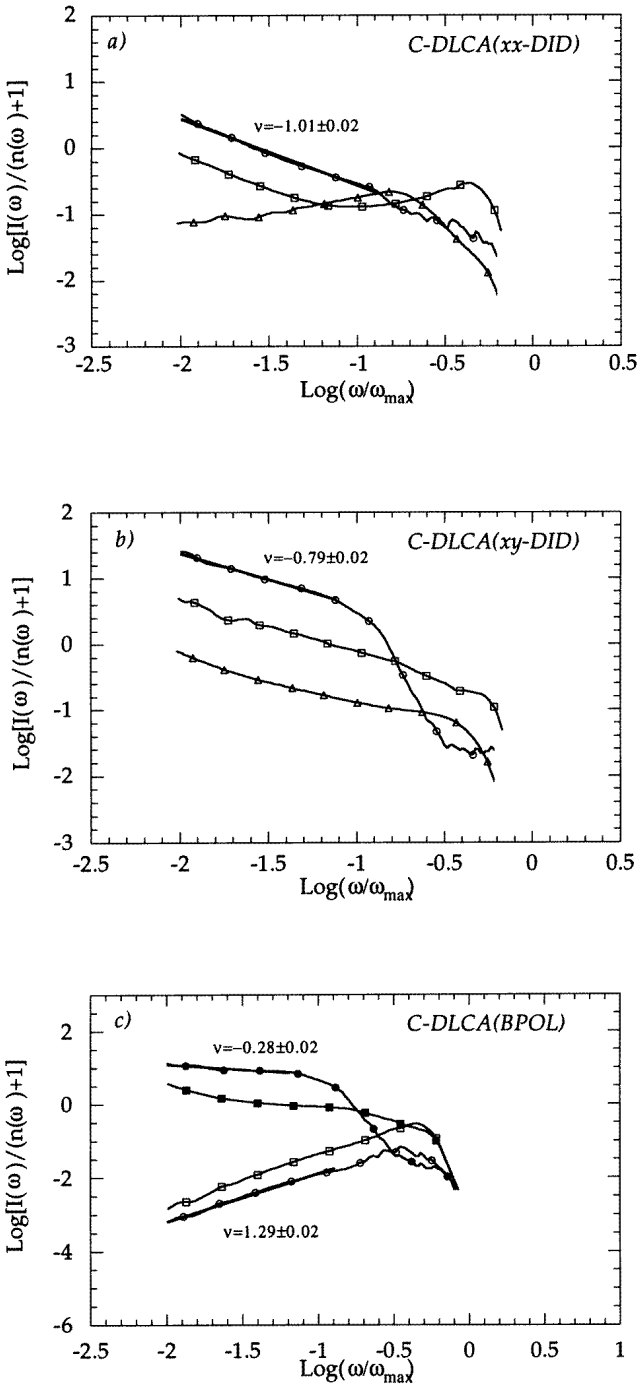

Figure 7. Log–log plot of Raman scattering intensity $I(\omega)/[n(\omega)+1]$ versus ω/ω_{max} for the C-DLCA system for tensorial elasticity for $\beta/\alpha = 0.01$ (○, ●), 0.10 (□, ■) and 1.00 (△): (*a*) *xx*-DID; (*b*) *xy*-DID; (*c*) *xx*-BPOL (○, □) and *xy*-BPOL (●, ■). ω_{max} is the maximal frequency of the spectra. The straight lines are fits with the indicated slopes.

$\beta/\alpha = 0.01$ (circles), 0.1 (squares) and 1.0 (triangles). In the case of the BPOL mechanism, the results for polarized (open symbols) and depolarized spectra (full symbols) are given for the values $\beta/\alpha = 0.01$ (circles) and 0.1 (squares). We observe that the scattering intensity exhibits scaling in a low-frequency region for the two mechanisms DID and BPOL. In table 2, we report the scaling exponents characterizing the low-frequency regime of scattered intensity, with $\beta/\alpha = 0.01$, for the BP and A-DLCA, B-DLCA and C-DLCA systems in the cases of polarized (depolarized) DID and BPOL mechanisms. These exponents are the slopes of the straight lines indicated in figures 5–7. For example, for sample B-DLCA, we obtain exponents $\nu = -1.01 \pm 0.02$ for xx-DID, $\nu = -0.80 \pm 0.02$ for xy-DID, $\nu = 1.33 \pm 0.02$ for xx-BPOL and $\nu = -0.34 \pm 0.02$ for xy-BPOL.

Table 2. The exponent ν, deduced from the spectrum, with the ratio $\beta/\alpha = 0.01$, in the case of the BP and DLCA vectorial models using DID and BPOL mechanisms.

	ν			
Model	xx-DID	xy-DID	xx-BPOL	xy-BPOL
BP	-1.03 ± 0.02	-0.93 ± 0.02	1.35 ± 0.02	
A-DLCA	-0.91 ± 0.02	-0.79 ± 0.02	1.35 ± 0.02	-0.40 ± 0.02
B-DLCA	-1.01 ± 0.02	-0.80 ± 0.02	1.33 ± 0.02	-0.34 ± 0.02
C-DLCA	-1.01 ± 0.02	-0.79 ± 0.02	1.29 ± 0.02	-0.28 ± 0.02

5. Discussion

5.1. Scalar model

For BP networks, we observe that, for both BPOL and DID mechanisms, the polarized and depolarized spectra are quite similar. Calculations of the scattering produced by the DID mechanism in BP networks revealed that, when the coherent strain was found to dominate, the Raman scattering intensity follows the scaling law (14), as predicted by Alexander *et al* (1993). From (14), one deduces, from xx-DID and xy-DID spectra, respectively, that the exponent σ is close to unity. Values obtained for the slopes are in agreement with those (with $m = \nu - \tilde{d} + 2$) obtained by Viliani *et al* (1995). Concerning the BPOL mechanism, the slopes are the same for both polarizations and also in agreement with those obtained by Viliani *et al* (1995).

With DLCAs, we observe that, for the DID mechanism, the slopes are different for the polarized and depolarized spectra and decrease as the concentration increases. On the other hand, it has been shown that the fractal dimension, spectral dimension and slopes of correlation functions in DLCA systems are identical for the three samples (Rahmani *et al* 1996). So, as the concentration increases, we observe a relative increase in the Raman 'inelastic structure factor' $a_{\alpha\gamma}(j)$ of the low-frequency modes. In fact, this factor depends on the real positions of all atoms which are different in the three samples. Furthermore, when comparing our results for DLCAs with equation (14), we deduce an exponent $\sigma \approx 0.50$ (xx-DID) and $\sigma \approx 0.39$ (xy-DID), which is extremely small and in disagreement with the scaling theory on Raman scattering given by Alexander *et al* (1993). Concerning the BPOL mechanism, the slopes are nearly independent of the concentration and are almost the same for both polarizations. With this mechanism, it is possible to compare our numerical results for DLCAs with equation (15). The slope in figure 2(c) gives $\nu \approx 0.77$. One can thus

deduce that $\sigma \approx 1.04$ in this case. This value is close to the value of the exponent $d_\phi \approx 1.0$ found in the experimental Raman scattering of some silica gels (Boukenter *et al* 1986).

Moreover, comparing our DID numerical results obtained for DLCAs with the experimental data on silica aerogels, we observe that, in the case of the scalar model, the Raman scattering intensity scales with an exponent $\nu \approx 0.26$–0.52. These values are consistent with the measured values in the 100–150 cm^{-1} range of the Raman spectra for these systems. We also note that the concentration-dependent variation on the exponent ν (table 2) is in agreement with experiments (Champagnon *et al* 1987).

5.2. Tensorial model

For BP networks, the behaviours of polarized and depolarized spectra produced by the DID mechanism are quite similar ($\nu(xx\text{-DID}) = -1.03 \pm 0.02$; $\nu(xy\text{-DID}) = -0.93 \pm 0.02$). It is obvious that we cannot compare our results with the formulae proposed by Alexander *et al* (1993) since it is difficult to establish the required scaling law.

With the DLCA system, we observe that, for the DID mechanism, slopes are slightly different for the polarized and depolarized spectra. For the xx-polarization, the slopes decrease as the concentration increases and are constant for the xy polarization. Note that, in contrast with the scalar models, the slopes are close to values obtained with BP networks. Concerning the BPOL mechanism, the slopes decrease slightly as the concentration increases and are very different for the two polarizations. Here again, the slopes are almost identical for xx-BPOL for BP networks and DLCAs.

It might be interesting to compare the results obtained with the DLCA model and the experimental results on silica aerogels. First, we note that, for DLCAs, the DOS of fractons in the low-frequency region is governed by a spectral dimension $\tilde{D} \approx 0.9$ which is close to that measured in base-catalysed silica aerogels, which are characterized by a fractal dimension $D \approx 1.70$–2.00. Second, the depolarized Raman scattering intensity was found to scale with $\nu \approx -0.79$ via the DID mechanism. This value agrees with the measured ν-value of about -0.72 to -0.85 for the depolarized scattering from the basic aerogels in the very-low-frequency region (Vacher *et al* 1990, Anglaret *et al* 1994). This supports the fact that the DLCA is a good model for basic aerogels, as we mentioned in previous studies (Hasmy *et al* 1994, Rahmani *et al* 1996).

In conclusion, taking into account the vectorial nature of interactions, we have shown that the DID mechanism applied to the DLCA model gives a good description of Raman scattering in base-catalysed silica aerogels. It would be interesting to extend the present study to other scattering mechanisms, such as the Pockels mechanism, to see whether the results are similar or not. We hope that these numerical probes with tensorial elasticity interactions will provide a basis for a new theoretical development on Raman scattering in fractal systems.

Acknowledgment

The computations were performed at the Centre National Universitaire Sud de Calcul (Montpellier, France) on an SP2 IBM computer.

References

Alexander S 1989 *Phys. Rev.* B **40** 7953
Alexander S, Courtens E and Vacher R 1993 *Physica* A **195** 286

Alexander S, Entin-Wohlman O and Orbach R 1985 *Phys. Rev.* B **32** 6447
——1986 *Phys. Rev.* B **33** 3935
Alexander S and Orbach R 1982 *J. Physique Lett.* **43** L625
Anglaret E, Hasmy A, Courtens E, Pelous J and Vacher R 1994 *Europhys. Lett.* **28** 591
Benoit C, Royer E and Poussigue G 1992a *J. Phys.: Condens. Matter* **4** 3125
Benoit C, Poussigue G and Assaf A 1992b *J. Phys.: Condens. Matter* **4** 3153
Boukenter A, Champagnon B, Dumas J, Duval E, Quinson J F and Serughetti J 1986 *Phys. Rev. Lett.* **57** 2391
——1987 *J. Non-Cryst. Solids* **95–96** 1189
Champagnon B, Duval E, Boukenter A, Serughetti J and Dumas J 1987 *Diffusion Defect Data* **53–4** 375
Courtens E, Pelous J, Phalippou J, Vacher R and Woignier T 1987 *Phys. Rev. Lett.* **58** 128
Courtens E, Vacher R, Pelous J and Woignier T 1988 *Europhys. Lett.* **6** 245
Feng S 1985a *Phys. Rev.* B **32** 510
——1985b *Phys. Rev.* B **32** 5793
Hasmy A, Anglaret A, Foret M, Pelous J and Jullien R 1994 *Phys. Rev.* B **50** 6006
Keys T and Ohtsuki T 1987 *Phys. Rev. Lett.* **59** 603
Mazzacurati V, Montagna M, Pilla O, Viliani G, Ruocco G and Signorelli G 1992 *Phys. Rev.* B **45** 2126
Montagna M, Pilla O, Viliani G, Mazzacurati V, Ruocco G and Signorelli G 1990 *Phys. Rev. Lett.* **65** 1136
Pelous J, Foret M and Vacher R 1992 *J. Non-Cryst. Solids* **145** 63
Pilla O, Viliani G, Montagna M, Mazzacurati V, Ruocco G and Signorelli G 1992 *Phil. Mag.* B **65** 243
Poussigue G, Benoit C, Sauvajol J L, Lere-Porte J P and Chorro C 1991 *J. Phys.: Condens. Matter* **3** 8803
Rahmani A, Benoit C, Jullien R, Poussigue G and Sakout A 1996 *J. Phys.: Condens. Matter* **8** 5555
Rahmani A, Benoit C and Poussigue G 1995 *J. Phys.: Condens. Matter* **7** 8903
Sahimi M and Arbabi S 1993 *Phys. Rev.* B **47** 703
Stoll E, Kolb M and Courtens E 1992 *Phys. Rev. Lett.* **68** 2472
Terao T and Nakayama T 1996 *Phys. Rev.* B **53** R2918
Tsujimi Y, Courtens E, Pelous J and Vacher R 1988 *Phys. Rev. Lett.* **60** 2757
Vacher R, Courtens E, Coddens G, Heidemann A, Tsujimi Y, Pelous J and Foret M 1990 *Phys. Rev. Lett.* **65** 1008
Vacher R, Woignier T, Pelous J and Courtens E 1988 *Phys. Rev.* B **37** 6500
Viliani G, Dell'Anna R, Pilia O and Montagna M 1995 *Phys. Rev.* B **52** 3346
Yakubo K and Nakayama T 1990 *Proc. Indian Acad. Sci.* **102** 581